DALTON
FULL PAPER

X-Ray crystallographic and extended X-ray absorption fine structure studies of gold(I) complexes containing weak intermolecular interactions

Peter Bishop,*[a] Patsy Marsh,[a] Alan K. Brisdon,[b] Brian J. Brisdon*[c] and Mary F. Mahon[c]

[a] *Cookson Matthey Technology Centre, Sandy Lane, Yarnton, Oxford, UK OX5 1PF*
[b] *Department of Chemistry, UMIST, PO Box 88, Manchester, UK M60 1QD*
[c] *School of Chemistry, University of Bath, Bath, UK BA2 7AY*

The crystal and molecular structures of $[Au_2\{S_2CN(C_2H_4OMe)_2\}_2]$, $[Au(PPh_3)(SCH_2CO_2H)]$, $[Au(PPh_3)(SCMe_2CO_2H)]$ and $[Au(PPh_3)(SCH_2CO_2Me)]$ have been determined. All compounds contain an approximately linear primary co-ordination sphere of ligands about the gold atom, but they differ markedly in their type of intermolecular interaction. In $[Au_2\{S_2CN(C_2H_4OMe)_2\}_2]$ the supramolecular array is dominated by an almost linear, polymeric backbone of gold atoms with alternate gold–gold contacts of 2.7902(6) (intramolecular) and 3.1572(7) Å (intermolecular), whereas in $[Au(PPh_3)(SCH_2CO_2H)]$ dimers associated through long gold–sulfur contacts of 3.131(2) Å are held together in a polymeric chain by hydrogen bonding between neighbouring carboxylic acid residues. The increased steric bulk of the thiolate ligand in $[Au(PPh_3)(SCMe_2CO_2H)]$ caused by the methyl groups on the α-carbon atom precludes association of the gold centres, but hydrogen bonding between carboxylates as in the SCH_2CO_2H compound causes dimerisation. Compound $[Au(PPh_3)(SCH_2CO_2Me)]$ exists as a monomer with no evidence of weak intermolecular interactions. Analysis of ambient-temperature EXAFS (extended X-ray absorption fine structure) measurements on solid samples of the first two compounds yield gold–gold separations of 2.775(2) and 3.271(6) Å and 4.188(15) Å, respectively. Gold–sulfur separations of 2.290(1) and 3.532(8) and of 2.329(4) and 3.124(19) Å, respectively, are also in good agreement with X-ray data.

Recent advances in gold chemistry have highlighted the flexible metal–metal bonding modes exhibited by this element.[1] Particular attention has been paid to compounds which contain weak intermolecular metal–metal interactions with gold–gold separations typically in the range 2.5–3.5 Å, which are intermediate between those found in the Au_2 molecule at 2.47 Å, and twice the gold van der Waals radius of 3.60 Å.[2] These attractive gold–gold interactions have been estimated to be as high as 30 kJ mol^{-1} in some compounds,[3] and they are considered to be significant in the stabilisation of hypervalent main group species such as $[C\{Au(PPh_3)\}_6]^{2+}$,[4] and of considerable utility in the self assembly and crystal engineering of gold-containing materials.[5]

Database analyses have revealed that gold–gold interactions are frequently observed in formally two-covalent gold(I) compounds containing auxiliary P- and/or S-donor ligands.[6] Gold–phosphine complexes are commonly used as reagents in organometallic chemistry,[7] and their potential as drugs for the treatment of rheumatoid arthritis has been explored in some detail.[8] Gold thiolates have also received attention as arthritis inhibitors and in chemotherapy,[9] and have been shown recently to possess important photophysical properties.[10] Therefore factors affecting the inter- and intra-molecular arrangements in such compounds are of considerable interest, and although theoretical studies of weak gold–gold bonding interactions are well developed,[11] they are insufficiently advanced to be used for predicting detailed structural information.

Experimental determinations of the internuclear parameters in gold cluster chemistry have depended almost exclusively upon single-crystal X-ray diffraction studies, and we are aware of only one previous investigation in which EXAFS (extended X-ray absorption fine structure) has been used very specifically to explore weak gold–gold interactions in the solid state.[12] As many potentially interesting and useful compounds in which such interactions might be important are polymeric, amorphous and insoluble, they are not amenable to X-ray single-crystal analysis. In this paper we explore the use of EXAFS as an alternative technique for this type of structural analysis, and show that, contrary to previous expectations,[12] weak gold–gold interactions involving internuclear distances greater than 3 Å can be determined from EXAFS signals measured at room temperature.

The study reported herein centres on four gold(I) compounds, each containing S-donor ligands which were functionalised with oxygen-containing substituents in order to increase their solubility in polar media. It forms part of a systematic investigation into the properties of gold thiolates. Single-crystal X-ray diffraction methods were used to reveal the differing structural features present in $[Au_2\{S_2CN(C_2H_4OMe)_2\}_2]$, $[Au(PPh_3)(SCH_2CO_2H)]$, $[Au(PPh_3)(SCMe_2CO_2H)]$ and $[Au(PPh_3)(SCH_2CO_2Me)]$, and EXAFS studies were carried out on the first two compounds in order to compare the internuclear separations obtained from these differing techniques.

Results and Discussion

Preparative methods for gold(I) dithiocarbamates

The first gold(I) dialkyldithiocarbamates were prepared by Akerstrom[13] by the careful reduction of gold(III) by sodium sulfite in saturated salt solution, followed by reaction with an aqueous solution of the sodium salt of the ligand. This method, and variations thereon, has been used to prepare a wide range of gold(I) dithiocarbamate complexes.[14–16] In the present study reduction to gold(I) was achieved using aqueous ethyl 2-hydroxyethyl sulfide as the reducing agent. The solution of the gold(I) intermediate so formed was added to an aqueous solution of the salt $K[S_2CN(C_2H_4OMe)_2]$ to afford solid $[Au_2\{S_2CN(C_2H_4OMe)_2\}_2]$, compound **1**, which was purified by extraction into chloroform. The spectroscopic features of **1** are in accord with data reported on analogues. It has been noted

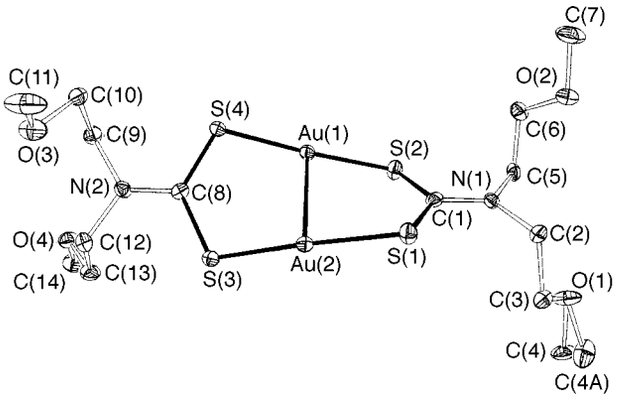

Fig. 1 Molecular structure of compound **1** showing the atom labelling scheme adopted. Thermal ellipsoids are drawn at the 30% probability level

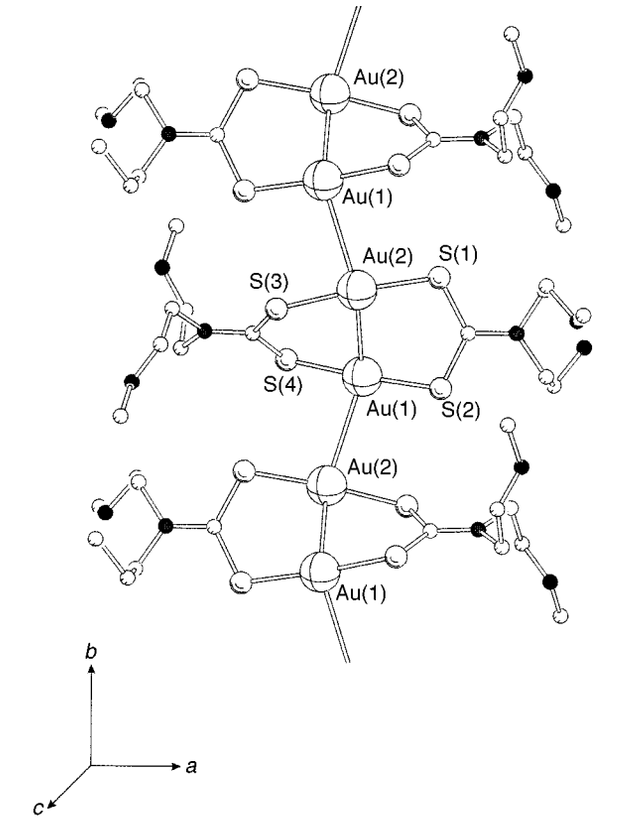

Fig. 2 Crystal packing diagram of compound **1** viewed down the *c* axis of the unit cell and showing the polymeric backbone of gold atoms in the direction of the *b* axis

previously that the infrared-active ν(C–N) mode is sensitive to both the chain length and the steric bulk of the alkyl substituent.[17] For this compound a value of 1494 cm^{-1} for this mode is very similar to that noted for gold(I) dialkyldithiocarbamates with short unbranched alkyl substituents R = Et (1496) or Pr (1490 cm^{-1}).[15] Crystals of **1** suitable for a single-crystal X-ray determination were grown from dichloromethane–methanol.

Gold(I) thiolates and their triphenylphosphine adducts

The homoleptic gold thiolates [Au(SCH_2CO_2H)] **2**, [Au($SCMe_2CO_2H$)] **4** and [Au(SCH_2CO_2Me)] **6** were prepared *via* reduction of gold(III) as for compound **1**, followed by addition of the thiol. The compounds were formed as yellow (**2** and **6**) and white (**4**) powders in nearly quantitative yields. Compound **2** has been cited previously[9] but was not fully characterised. The polymeric nature of most homoleptic gold(I) thiolates results in poor solubility, and as a result only [{2,4,6-$Pr^i_3C_6H_2S$)Au}$_6$] has been fully characterised by X-ray crystallographic methods.[18] The thiolates reported in this study also exhibited very low solubilities in either water or organic solvents, but both **2** and **4** dissolved sufficiently in D_2O containing NaOD for the collection of ^{1}H NMR data, as noted in the Experimental section.

The alcohol-soluble gold thiolates [Au(PPh_3)(SCH_2CO_2H)] **3**, [Au(PPh_3)($SCMe_2CO_2H$)] **5** and [Au(PPh_3)(SCH_2CO_2Me)] **7** were prepared by heating the gold thiolates **2**, **4** or **6** under reflux with 1 equivalent of triphenylphosphine in ethanol. Previous workers[19–21] have prepared phosphine adducts of gold(I) thiolates by an alternative route which involves the reaction of halogeno(tertiary phosphine)gold(I) compounds with 1 equivalent of thiol in the presence of base. The method used in this study affords clean products in high yields and avoids any possible complications caused by using basic solutions of thiols. Compounds **2**, **4** and **6** were characterised by IR, ^{1}H and ^{31}P NMR spectroscopies and elemental analyses. The ^{31}P chemical shift data are similar to those reported for other P–Au–S containing analogues,[20,21] suggesting that the phosphorus environment is only slightly dependent upon the nature of the sulfur ligand attached to gold.

Crystals of compounds **3**, **5** and **7** suitable for structure determinations were grown from hot ethanol, hot Pr^iOH and ethanol respectively.

Table 1 Selected bond lengths (Å) and angles (°) for complex **1**

Au(1)–S(2)	2.289(2)	S(1)–C(1)	1.736(9)
Au(1)–S(4)	2.292(2)	S(2)–C(1)	1.742(9)
Au(1)–Au(2)	2.7902(6)	S(3)–C(8)	1.732(8)
Au(1)–Au(2′)	3.1572(7)	S(4)–C(8)	1.723(9)
Au(2)–S(3)	2.296(2)	N(1)–C(1)	1.331(10)
Au(2)–S(1)	2.300(2)	N(2)–C(8)	1.323(10)
S(2)–Au(1)–S(4)	174.58(9)	Au(1)–Au(2)–Au(1″)	147.35(2)
S(2)–Au(1)–Au(2)	90.67(6)	C(1)–S(1)–Au(2)	109.1(3)
S(4)–Au(1)–Au(2)	88.70(6)	C(1)–S(2)–Au(1)	110.0(3)
S(2)–Au(1)–Au(2′)	98.44(6)	C(8)–S(3)–Au(2)	107.6(3)
S(4)–Au(1)–Au(2′)	85.35(6)	C(8)–S(4)–Au(1)	107.3(3)
Au(2)–Au(1)–Au(2′)	141.49(2)	N(1)–C(1)–S(1)	116.9(7)
S(3)–Au(2)–S(1)	173.58(9)	N(1)–C(1)–S(2)	116.5(6)
S(3)–Au(2)–Au(1)	86.90(6)	S(1)–C(1)–S(2)	126.6(5)
S(1)–Au(2)–Au(1)	91.68(6)	N(2)–C(8)–S(4)	117.7(6)
S(3)–Au(2)–Au(1″)	86.23(6)	N(2)–C(8)–S(3)	117.3(6)
S(1)–Au(2)–Au(1″)	98.26(6)	S(4)–C(8)–S(3)	124.9(5)

Primed and double primed atom positions are related to corresponding unprimed atoms by the $-x+\frac{1}{2}, y-\frac{1}{2}, -z+\frac{1}{2}$ and $-x+\frac{1}{2}, y+\frac{1}{2}, -z+\frac{1}{2}$ symmetry operations respectively.

Crystal structures

The crystal structure of compound **1** consists of two gold(I) atoms in a slightly puckered eight-membered ring composed of two gold, four sulfur and two carbon atoms (Fig. 1). Each gold atom is co-ordinated to two sulfur atoms [Au(1)–S(2) 2.289(2), Au(1)–S(4) 2.292(2), Au(2)–S(3) 2.296(2), Au(2)–S(1) 2.300(2) Å], one from each bridging ligand, so achieving almost linear co-ordination with S(2)–Au(1)–S(4) 174.58(9)° and S(1)–Au(2)–S(3) 173.58(9)° (Table 1). In addition to a short intramolecular gold–gold separation of 2.7902(6) Å, molecules are linked by longer intermolecular gold–gold interactions [3.1572(7) Å], so generating a supermolecular array dominated by a polymeric backbone of gold atoms (Fig. 2). Both [$Au_2(S_2CNPr^i_2)_2$] and [$Au_2(S_2CNBu_2)_2$] have been shown to exhibit similar structural features,[22,23] but with a much longer gold–gold intermolecular interaction of 3.40 Å in the former complex.[22]

The structure of compound **3** can also be described as a supermolecular array displaying weak inter- and intramolecular associations, but neither involves gold–gold interactions. Instead two alternative structural features are evident

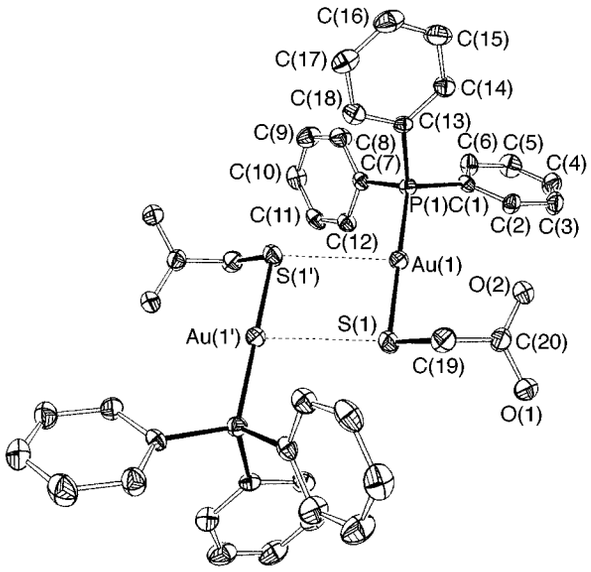

Fig. 3 Molecular structure of compound **3** showing the atom labelling scheme used, and the interactions between neighbouring molecules *via* gold–sulfur contacts around an inversion centre. Thermal ellipsoids as in Fig. 1

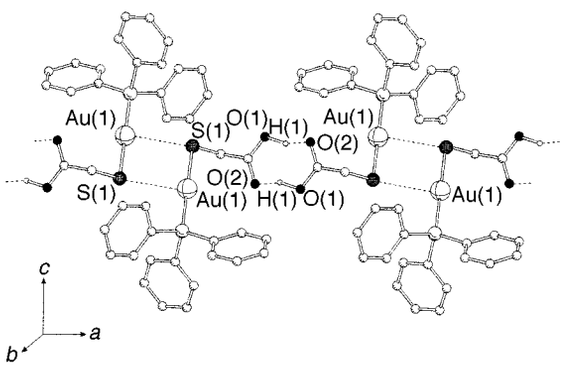

Fig. 4 Crystal packing diagram of compound **3** viewed down the *b* axis showing the two forms of intermolecular association along the *a* axis. Hydrogen atoms, which were included in calculated positions except for the carboxylic acid proton H(1), have been omitted for clarity. The atom H(1) was located and refined at a fixed distance of 0.9 Å from O(1)

Table 2 Selected bond lengths (Å) and angles (°) for compound **3**

Au(1)–P(1)	2.254(2)	Au(1)···S(1′)	3.131(2)
Au(1)–S(1)	2.308(2)	S(1)–C(19)	1.815(10)
P(1)–Au(1)–S(1)	178.85(8)	Au(1)–S(1)–Au(1′)	93.45(8)
S(1)–Au(1)–S(1′)	86.55(8)	C(19)–S(1)–Au(1)	105.1(3)

Primed atom positions are related to corresponding unprimed atoms by the $-x, -y, -z$ symmetry operation.

(Figs. 3 and 4, Table 2). First, neighbouring pairs of molecules in which each gold atom is co-ordinated approximately linearly [178.85(8)°] by one sulfur atom [2.308(2) Å] and one phosphorus atom [2.254(2) Å] interact with each other in a 'head to tail' arrangement *via* sulfur–gold contacts around an inversion centre [Au(1)···S(1′) 3.131(2) Å, S(1)–Au(1)–S(1′) 86.55(8), Au(1)–S(1)–Au(1′) 93.45(8)°]. Secondly, the carboxylate groups of neighbouring molecules are hydrogen bonded [H(1)–O(2) 1.41(3) Å, O(1)–H(1)–O(2) 162.7°]. These two categories of alternating intermolecular contacts produce a one-dimensional polymeric backbone which dominates the supramolecular array (Fig. 4).

Molecular models indicate that on increasing the bulk of the thiolate ligand the large steric bulk of the triphenylphosphine

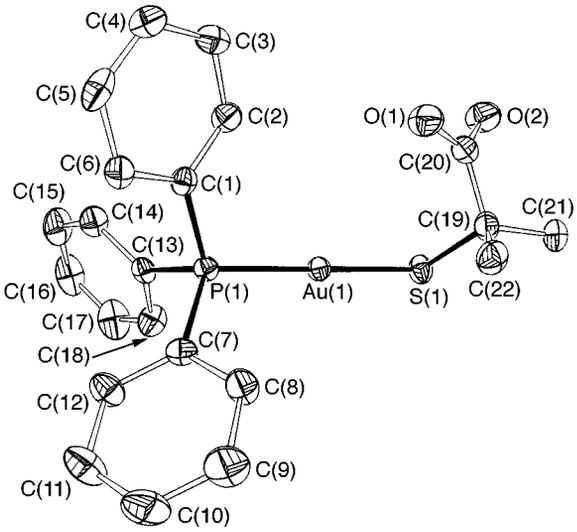

Fig. 5 Molecular structure of compound **5** showing the atom labelling scheme adopted. Thermal ellipsoids as in Fig. 1

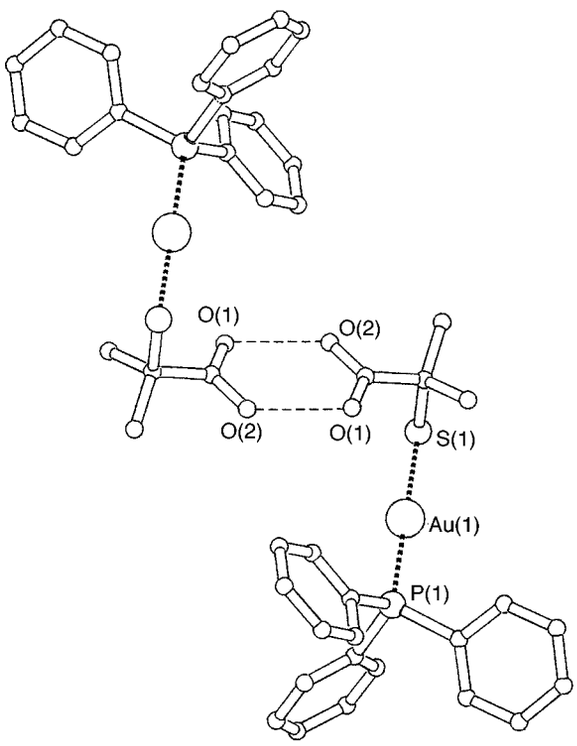

Fig. 6 Crystal packing diagram of compound **5** showing dimer formation. The carboxylic acid proton was not located

Table 3 Selected bond lengths (Å) and angles (°) for compound **5**

Au(1)–P(1)	2.2582(14)	S(1)–C(19)	1.848(6)
Au(1)–S(1)	2.2896(14)		
P(1)–Au(1)–S(1)	179.34(5)	C(19)–S(1)–Au(1)	104.8(2)

ligand will prevent the form of association noted in compound **3** above. To investigate this, the crystal structure of [Au(PPh_3)-($SCMe_2CO_2H$)] **5** was determined with the result illustrated in Figs. 5 and 6. Unlike the previous two structures, the gold atom is strictly two-co-ordinate [P(1)–Au(1)–S(1) 179.34(5)°], with gold–sulfur and –phosphorus bond lengths of 2.2896(14) and 2.2582(14) Å respectively (Table 3). Dimers are formed from hydrogen bonding between pairs of carboxylate residues. Although the acid proton could not be located with certainty,

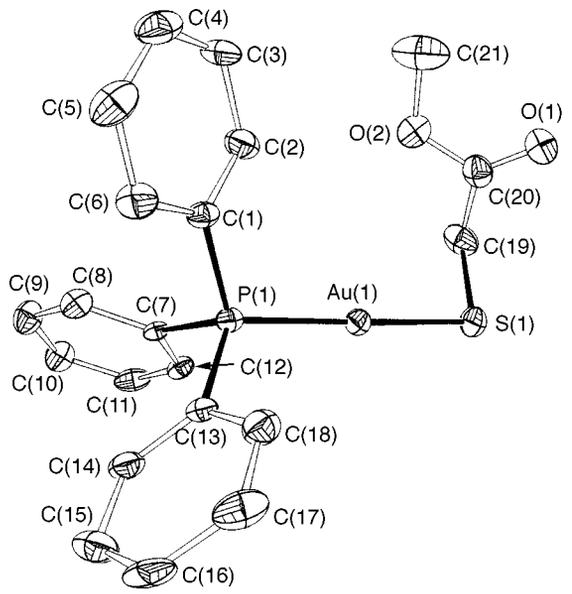

Fig. 7 Molecular structure of compound **7** showing the atom labelling scheme adopted. Thermal ellipsoids as in Fig. 1

Table 4 Selected bond lengths (Å) and angles (°) for compound **7**

Au(1)–P(1)	2.265(2)	S(1)–C(19)	1.848(12)
Au(1)–S(1)	2.298(2)		
P(1)–Au(1)–S(1)	178.96(8)	C(19)–S(1)–Au(1)	101.3(3)

the O(1)···O(2) separation at 2.605(6) Å in **5** is very similar to that found in compound **3** and in [Au(CNBu)($SC_6H_4CO_2H$)].[24] The lack of associative interactions between gold centres has no appreciable effect upon either the gold–phosphorus separations or the Au–S–C angle, but it does appear to modify the gold–sulfur bond length. Thus in **5** the latter is significantly shorter than the corresponding distance noted in **3** [2.308(2) Å].

Although compound **7** is the methyl ester of **3** it shows no tendency to associate intermolecularly. The Au(1)–P(1) and Au(1)–S(1) separation at 2.265(2) and 2.298(2) Å respectively are very similar to those in **3**, and the molecule shows a very similar P–Au–S arrangement (Fig. 7, Table 4). The most notable structural differences between the two complexes occur within the thiolate ligands, but these are small. In **7** the Au(1)–S(1)–C(19) angle at 101.3(3) is approximately 4° less than the corresponding angle in **3**, and the S(1)–C(19) separation at 1.848(12) Å may be slightly longer than in the free acid analogue. Nevertheless these parameters are well within the range of values observed for other complexes of this type,[21–23] and there seems no obvious steric reason why **7** does not dimerise. It has been suggested recently[21] that, in the absence of steric hindrance or solvent molecules, complexes LAuX (with L a neutral donor ligand and X an anionic group) are generally found as aggregates with close gold–gold contacts regardless of the nature of L and X. In the structures of **3**, **5** and **7** discussed above we have noted an extremely subtle interplay of weak interactions involving gold–gold, gold–sulfur, hydrogen-bonding, and van der Waals forces, which provide some interesting exceptions to this generalisation.

EXAFS Studies

The EXAFS measurements were carried out on compounds **1** and **3**, both of which exhibit short- and long-range heavy-atom interactions. This is a powerful technique for analysing the local environment about a specific atom, and has been used very successfully to detect relatively strong interactions at room temperature.[25,26] However weaker interactions, especially those

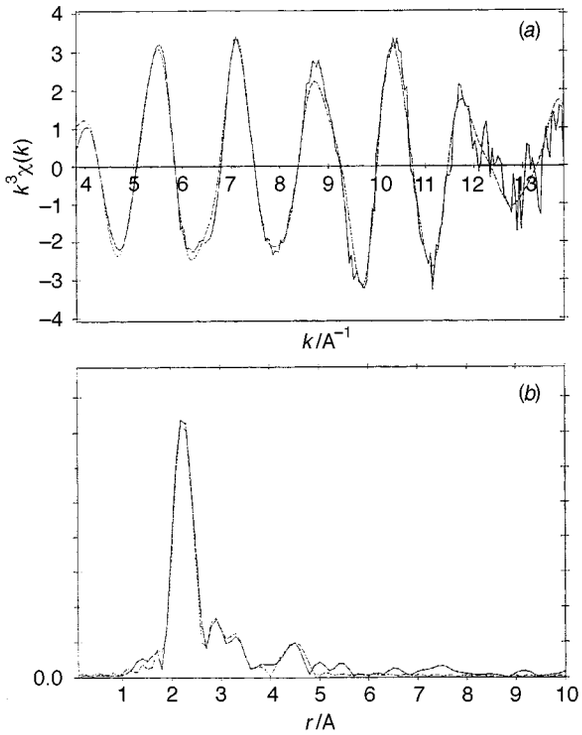

Fig. 8 (*a*) Background-subtracted gold L(III)-edge EXAFS spectra for compound **1** (——, experimental × k^3; – – –, curved-wave theory × k^3), and (*b*) corresponding Fourier-transform magnitudes in arbitrary units (——, experimental; – – –, theoretical)

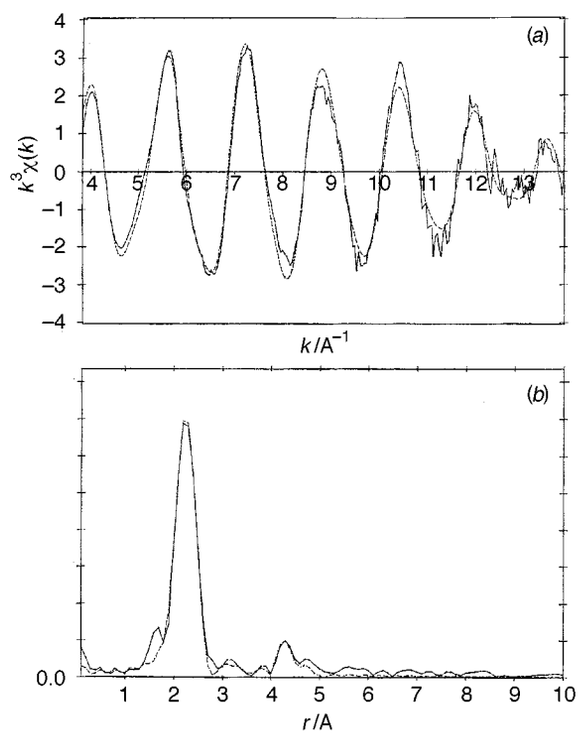

Fig. 9 (*a*) Background-subtracted gold L(III)-edge EXAFS spectra for compound **3**. Details as in Fig. 8

giving rise to an atom separation of over 3 Å, have been less frequently detected at room temperature by EXAFS due to thermal disorder which dampens the signal amplitude.[12] We are aware of only two early reports[27] in gold chemistry where attempts were made to extract this type of structural information from room-temperature EXAFS data, and for the two compounds studied there were no comparative X-ray data available for corroboration of the EXAFS results. In this study gold L(III) EXAFS spectra were recorded at room temperature

Table 5 Comparative data for EXAFS and X-ray crystallographic analyses of compounds **1** and **3**

Compound	Shell	Distance[a]/Å	$2\sigma^2$[b]/Å^{-2}	X-Ray distance[c]/Å	R[d] (%)
1	Au–S	2.290(1)	0.005(1)	2.294	17.9
	Au–Au	2.775(2)	0.008(2)	2.790	
	Au · · · Au	3.271(6)	0.015(3)	3.157	
	Au · · · S	3.532(8)	0.008(2)	3.569	
3	Au–S	2.329(4)	0.001(1)	2.308	18.9
	Au–P	2.232(4)	0.001(1)	2.254	
	Au · · · S	3.124(19)	0.039(5)	3.131	
	Au · · · Au	4.188(15)	0.012(3)	4.001	

[a] Standard deviation in parentheses; systematic errors in bond distances arising from data collection and analysis procedures are *ca.* 0.02 Å. [b] Debye–Waller factor. [c] Averaged values. [d] $R = [(\chi^{theory} - \chi^{exptl})k^3 dk/\chi^{exptl} k^3 dk] \times 100$.

in transmission mode out to $k = 15$ Å^{-1}, where k = the photoelectron wavevector, on samples prepared as finely ground solids mulled with boron nitride. The results were analysed using standard procedures.[28,29] The contributions due to long-distance heavy-atom interactions dominate the EXAFS spectra at >10 k and therefore several data sets were collected and averaged for each compound, and the averaged data multiplied by k^3 to compensate for the fall-off in intensity at higher k values. However, due to poor signal-to-noise ratio the data sets were truncated at $k = 14$ Å^{-1} rather than smoothing or Fourier filtering the data.

The Fourier transform of the background-subtracted EXAFS data for compound **1** (Fig. 8) is dominated by a single broad peak at *ca.* 2.3 Å with additional weaker features at around 2.8, 3.3 and 4.5 Å. The Fourier transform for **3** is similarly dominated by a peak at 2.3 Å, but it has just one other distinct feature at around 4.2 Å (Fig. 9).

Analysis of the data for compound **1** was undertaken initially using a single-shell model consisting of two ligated sulfur atoms. Iteration of this model resulted in a Au–S separation of 2.291 Å and a R factor of just under 30%. This value could only be improved significantly by including a second shell corresponding to another gold atom at a distance of *ca.* 2.8 Å. Iteration of this model resulted in a Au–Au distance of 2.78 Å and a R factor of 20%, so defining the primary co-ordination sphere of the gold atoms. Addition of shells corresponding to weak or non-bonded contacts between heavy atoms (Au · · · Au, Au · · · S) afforded further improvement to R resulting in a final value of 17.8%. Attempts were made to model Au · · · Au shells as Au · · · S shells. This resulted in significantly worse fits for **1** and negative Debye–Waller factors for **3**. On this basis we conclude that the back scattering arising from the heavy gold atoms and the other much lighter atoms in the molecules can be distinguished. The addition of each successive shell was tested for statistical significance using the procedure of Joyner *et al.*[30] Only shells which passed at the 1% significance level are included in the final model. In all cases the addition of non-bonded shells resulted in a decrease in the R factor whilst the distance of the bonded shells remained essentially invariant.

Two procedures were used to check on the shell co-ordination numbers used in the initial modelling. In the first the occupancy of the shells was included in the final iteration process, and in the second the occupation number for each shell was mapped against its Debye–Waller factor. Neither of these produced a change in any co-ordination number. The final set of parameters obtained for compound **1** is listed in Table 5 which also contains the corresponding X-ray data.

Initial modelling for the data on compound **3** was undertaken based on a two-shell model containing one S and one P atom. Both of these contributions are contained within the single broad envelope seen in the Fourier transform. Modelling of the data in terms of these two shells alone yielded an R factor of 22% with Au–S and Au–P separations of 2.33 and 2.23 Å respectively. On reversing the order of these shells a slight increase in the value of the R factor resulted, although it is not surprising that there is some difficulty in distinguishing clearly between these two shells in view of the similar distances and electronic configuration of the back-scattering atoms. A decrease in the R factor was only obtained when more distant shells corresponding to non-bonded atoms were included in the modelling. There is no signal at around 2.8 Å corresponding to a direct Au–Au interaction as occurs in **1**. This is in accord with the X-ray data which showed a completely different structural arrangement in the two compounds. The next most obvious shell in **1** is located at around 4.2 Å and including this as a shell of gold atoms [corresponding to a non-bonded Au(1) · · · Au(1′) separation], followed by iteration, resulted in a decrease in the R factor. Inclusion of shells of non-bonded Au–S and Au–C atoms at *ca.* 3.1 and 4.2 Å respectively in the final modelling of the data resulted in a final R factor of 18.9%. All shells in the final model passed the significance test at the 1% level. The data in Table 5 refer to all gold–heavy atom separations in the range 0–4 Å obtained for **1** and **3** by both methods of structural analysis. The close correspondence of the two sets of data bears testimony to the potential of EXAFS as a structural tool for the evaluation of close and distant contacts between heavy atoms corresponding to both strong *and* weak interactions, especially for compounds whose structures cannot be evaluated using single-crystal X-ray methods.

Experimental

All solvents were dried and purified using standard procedures.[31] Sodium tetrachloroaurate dihydrate, sulfanylacetic acid, ethyl 2-hydroxyethyl sulfide, bis(2-methoxyethyl)amine, carbon disulfide, potassium hydroxide and triphenylphosphine were reagent grade and used as commercially supplied. The thiol $HSCMe_2CO_2H$ was synthesized following literature procedures.[32] Infrared spectra were recorded on a Perkin-Elmer P-E 1720X FT-IR spectrometer using KBr discs, proton, carbon and phosphorus NMR spectra on a JEOL GSX 270 machine with shifts reported as δ values (ppm) relative to an internal $SiMe_4$ standard. Elemental analyses were performed by the Department of Pure and Applied Chemistry, University of Strathclyde.

Syntheses

$K[S_2CN(C_2H_4OMe)_2]$. Potassium hydroxide (4.20 g, 0.076 mol) was stirred with $(MeOCH_2)_2NH$ (6.25 g, 0.05 mol) in acetone (200 cm^3) whilst cooled in ice. Carbon disulfide (5 cm^3, excess) in acetone (20 cm^3) was added and the reaction flask stoppered. Stirring for 3.5 h resulted in an orange solution and some unchanged potassium hydroxide which was filtered off. Addition of diethyl ether (500 cm^3) to the filtrate afforded a pale cream solid. This was collected and recrystallised from hot propan-2-ol to give a pale cream microcrystalline product. Yield 8.03 g, 65% (Found: C, 34.1; H, 5.9; N, 5.65. $C_7H_{14}KNO_2S_2$ requires C, 34.0; H, 5.7; N, 5.7%). $\tilde{\nu}_{max}$/cm^{-1} (in KBr) 1495s (CN), 983 (CS). $\delta_H(D_2O)$ 3.38 (s, 6 H, OMe), 3.79 (t, 4 H) and 4.28 (t, 4 H).

Table 6 Crystallographic data for compounds **1**, **3**, **5** and **7**

Complex	**1**	**3**	**5**	**7**
Empirical formula	$C_{14}H_{28}Au_2N_2O_4S_4$	$C_{20}H_{18}AuO_2PS$	$C_{22}H_{22}AuO_2PS$	$C_{21}H_{20}AuO_2PS$
M	810.56	550.34	578.39	564.37
Crystal system	Monoclinic	Orthorhombic	Monoclinic	Monoclinic
Space group	$P2_1/n$	*Pbca*	$P2_1/n$	$P2_1/n$
a/Å	14.612(2)	11.575(1)	8.732(1)	14.705(2)
b/Å	10.774(2)	15.346(2)	17.988(4)	8.0370(10)
c/Å	14.678(2)	21.688(3)	13.938(3)	17.385(3)
β/°	101.88(2)	—	95.28(2)	98.48(1)
U/Å^3	2261.3(6)	3852.4(8)	2180.0(7)	2032.2(5)
Z	4	8	4	4
D_c/g cm^{-3}	2.381	1.898	1.762	1.845
μ(Mo-Kα)/mm^{-1}	13.351	7.839	6.93	7.433
F(000)	1520	2112	1120	1088
Crystal size/mm	0.2 × 0.2 × 0.2	0.2 × 0.2 × 0.25	0.15 × 0.15 × 0.2	0.2 × 0.2 × 0.25
No. data collected	3499	2963	3640	3166
Maximum, minimum transmission	1.000, 0.497	1.000, 0.477	1.17, 0.80*	1.000, 0.285
Data, restraints, parameters	3496, 0, 248	2952, 1, 230	3398, 0, 247	3166, 0, 237
Goodness of fit	1.101	1.149	0.776	0.815
*R*1, *wR*2 [$I > 2\sigma(I)$]	0.0295, 0.0641	0.0332, 0.0532	0.0226, 0.0637	0.0287, 0.0925
(all data)	0.0572, 0.0742	0.0969, 0.0721	0.0418, 0.0714	0.0493, 0.1162
Maximum, minimum residual electron density/e Å^{-3}	1.129, −0.748	0.671, −0.586	0.848, −0.606	0.747, −0.505
Weighting scheme, w^{-1}, where $P = (F_o^2 + 2F_c^2)/3$	$\sigma^2(F_o^2) + (0.0362P)^2 + 8.2330P$	$\sigma^2(F_o^2) + (0.0060P)^2 + 18.8583P$	$\sigma^2(F_o^2) + (0.0699P)^2 + 0.0496P$	$\sigma^2(F_o^2) + (0.1173P)^2 + 0.1860P$
Extinction coefficient	0.001 09(15)	—	0.000 42(15)	0.0009(3)

Details in common: λ(Mo-Kα) 0.709 30 Å; $T = 293(2)$ K; θ range 2–24°. * Maximum and minimum absorption corrections quoted.

[$Au_2\{S_2CN(C_2H_4OMe)_2\}_2$] 1. Sodium tetrachloroaurate dihydrate (5.00 g, 12.6 mmol) was dissolved in water (150 cm^3) and added dropwise to a stirred solution of ethyl 2-hydroxyethyl sulfide (4.00 g, 37.7 mmol). When the solution became colourless it was added to $K[S_2CN(C_2H_4OMe)_2]$ (3.40 g, 13.8 mmol) dissolved in water (50 cm^3). Addition of chloroform (50 cm^3) dissolved the resulting sticky yellow precipitate. The chloroform layer was removed from the aqueous solution and allowed to stand overnight, which resulted in the deposition of fine luminescent needles. These were collected, washed with methanol and dried *in vacuo*. Yield 3.68 g, 72.4% (Found: C, 20.7; H, 3.5; N, 3.4. $C_{14}H_{28}Au_2N_2O_4S_4$ requires C, 20.7; H, 3.5; N, 3.5%). $\tilde{\nu}_{max}/cm^{-1}$ 1494s (CN), 1009, 984 (CS). $\delta_H(CDCl_3)$ 3.36 (s, 6 H, OMe), 3.75 (t, 4 H) and 4.22 (t, 4 H).

[$Au(SCH_2CO_2H)$] 2. A solution of sodium tetrachloroaurate dihydrate (23.9 g, 0.060 mol) in water (150 cm^3) was added dropwise with stirring to ethyl 2-hydroxyethyl sulfide in water (100 cm^3). Stirring was continued until the solution had decolourised indicating reduction of Au^{III} to Au^{I}. Sulfanylacetic acid (6.07 g, 0.066 mol) in water (150 cm^3) was added carefully to the reaction vessel. An off-white emulsion was immediately formed but on continued stirring a yellow gelatinous precipitate resulted. This was filtered off, washed with water, ethanol and finally diethyl ether, and dried overnight at 50 °C to give a bright yellow powder. Yield 16.8 g, 97% (Found: C, 8.55; H, 1.1. $C_2H_3AuO_2S$ requires C, 8.3; H, 1.05%). $\tilde{\nu}_{max}/cm^{-1}$ 3446 (br) (OH), 1689s (CO) and 327w (Au–S). $\delta_H(D_2O$ in the presence of NaOD) 3.30 (br, CH_2).

[$Au(PPh_3)(SCH_2CO_2H)$] 3. Compound **2** (1.00 g, 3.47 mmol) was heated under reflux in ethanol (100 cm^3) with triphenylphosphine (0.91 g, 3.47 mmol). The colourless solution so formed was cooled resulting in the formation of a white crystalline product which was collected, washed with ethanol and diethyl ether, and dried *in vacuo*. Yield 1.47 g, 77% (Found: C, 43.7; H, 3.0. $C_{20}H_{18}AuO_2PS$ requires C, 43.6; H, 3.3%). $\tilde{\nu}_{max}/cm^{-1}$ 3447 (br) (OH) and 1684s (CO). $\delta_H(CD_3OD)$ 3.50 (s, 2 H, CH_2) and 7.50–7.59 (m, 15 H, aromatics). $\delta_P(CD_3OD)$ 39.3.

[$Au(SCMe_2CO_2H)]\cdot H_2O$ 4. Reaction of sodium tetrachloroaurate (2.00 g, 0.010 mol), ethyl 2-hydroxyethyl sulfide (2.66 g, 0.025 mol) and dimethylsulfanylglycolic acid (1.32 g, 0.011 mol) using a similar method to that for compound **2** above, resulted in the formation of the product as a white powder, 2.94 g, 93% (Found: C, 14.4; H, 3.1; S, 9.6. $C_4H_9AuO_3S$ requires C, 14.4; H, 2.7; S, 9.6%). $\tilde{\nu}_{max}/cm^{-1}$ 3447 (br) (OH) and 1694s (CO). $\delta_H(D_2O$ in the presence of NaOD) 1.70 (s, Me).

[$Au(PPh_3)(SCMe_2CO_2H)$] 5. Compound **4** (0.50 g, 1.58 mmol) was heated under reflux in ethanol (100 cm^3) with triphenylphosphine (0.41 g, 1.58 mmol) for 1.5 h. The resulting colourless solution was left to cool and the solvent then evaporated to leave a white oil. Trituration with diethyl ether produced a white microcrystalline powder which was collected and washed with more diethyl ether before being dried. Recrystallisation from hot ethanol afforded crystals of suitable quality for a single-crystal X-ray study. Yield 0.84 g, 92% (Found: C, 45.7; H, 3.8. $C_{22}H_{22}AuO_2PS$ requires C, 45.7; H, 3.8%). $\tilde{\nu}_{max}/cm^{-1}$ 3447 (br) (OH) and 1676 (CO). $\delta_H(CD_3OD)$ 1.64 (s, 6 H, Me) and 7.50 (m, 15 H, aromatics). $\delta_P(CD_3OD)$ 39.6.

[$Au(SCH_2CO_2Me)$] 6. Reaction of sodium tetrachloroaurate (6.00 g, 15.1 mmol), ethyl 2-hydroxyethyl sulfide (4.00 g, 37.7 mmol) and $HSCH_2CO_2Me$ (1.85 g, 16.6 mmol) using a similar method to that for compound **2** above afforded the product as a pale yellow powder which was filtered off, washed with solvent and dried. Yield 4.05 g, 89% (Found: C, 12.0; H, 1.50. $C_3H_5AuO_2S$ requires C, 11.9; H, 1.70%). $\tilde{\nu}_{max}/cm^{-1}$ 1730 (CO).

[$Au(PPh_3)(SCH_2CO_2Me)$] 7. Compound **6** (1.00 g, 3.30 mmol) was heated under reflux with triphenylphosphine (0.87 g, 3.30 mmol) and ethanol (120 cm^3) for 1.5 h. Ethanol was removed from the cooled solution to afford a viscous oil which was dissolved in a little diethyl ether. Careful addition of hexane produced a white microcrystalline product which was separated, washed with hexane and dried. Recrystallisation from hot propan-2-ol gave fine white needles of **7**. Yield 1.38 g, 74% (Found: C, 44.9; H, 3.80. $C_{21}H_{20}AuO_2PS$ requires C, 44.7; H, 3.55%). $\tilde{\nu}_{max}/cm^{-1}$ 1732 (CO) and 338 (Au–S). $\delta_H[(CD_3)_2CO]$ 3.48 (s, 2 H, CH_2), 3.58 (s, 3 H, Me) and 7.54–7.70 (m, 15 H, aromatics). $\delta_P[(CD_3)_2CO]$ 40.0.

X-Ray crystallography

Many of the details of the structure analyses carried out on compounds **1**, **3**, **5** and **7** are summarised in Table 6. All measurements were made on a CAD4 automatic four-circle diffractometer, and data were corrected for Lorentz, polarisation and absorption[33] throughout. Data for **1**, **5** and **7** were also corrected for extinction. Structures were solved and refined using SHELX 86[34] and SHELXL 93.[35] Refinements were based on F^2 for all complexes except **5**, where F data were used. Full-matrix least-squares anisotropic refinements were implemented in all cases. The asymmetric units of **1**, **3**, **5** and **7** shown in the figures (unprimed numbers) were produced using ORTEX.[36] Hydrogen atoms were included at calculated positions where relevant except on disordered carbon C(4) in **1**, which shared a site occupancy of 1 with position C(4A) in the ratio 58:42. Unfortunately the acidic proton in **5** could not be located with certainty.

CCDC reference number 186/813.

EXAFS Measurements

The EXAFS studies were carried out on finely divided mixtures of the compound and boron nitride (Aldrich) in the approximate ratio 1:10 packed into a 1 mm thick aluminium spacer and held in place using sticky tape. The gold L(III)-edge transmission spectra were recorded at the Daresbury Synchrotron Radiation Source operating at 2 GeV (*ca.* 3.2×10^{-10} J) with an average operating current of 210 mA on station 9.2 using a Si(220) monochromator offset to 50% of the rocking curve for harmonic rejection. Three data sets were collected at room temperature in k space and averaged to improve the signal-to-noise ratio. No sample decomposition was detected during the experiment. Calibration of the monochromator position was carried out using thin gold foil. The EXAFS data treatment utilised the programs EX[27] and EXCURV 92.[28] The background was removed by fitting the pre-edge by a straight line and subtracting this from the spectrum. The atomic contribution to the oscillatory part of the absorption spectrum was approximated using a high-order polynomial and the optimum fit judged by minimising the intensity of chemically insignificant shells at low r in the Fourier transform. Curve fitting to the background-subtracted data used single-scattering curve-wave theory, with phase shifts and back scattering calculated using the default *ab initio* method within EXCURV 92.

Acknowledgements

We thank the Director of the Daresbury Laboratory for the provision of facilities.

References

1 D. M. P. Mingos, *J. Chem. Soc.*, *Dalton Trans.*, 1996, 561; H. Schmidbaur, *Gold Bull.*, 1990, **23**, 11; *Chem. Soc. Rev.*, 1995, 391.
2 A. Bondi, *J. Phys. Chem.*, 1964, **68**, 441.
3 H. Schmidbaur, W. Graf and G. Müller, *Angew. Chem.*, *Int. Ed. Engl.*, 1988, **27**, 417.

4 H. Schmidbaur, *Pure Appl. Chem.*, 1993, **65**, 691; F. Scherbaum, A. Grohmann, B. Huber, C. Kruger and H. Schmidbaur, *Angew. Chem., Int. Ed. Engl.*, 1988, **27**, 1544.
5 A. Ulman, *Chem. Rev*, 1996, **96**, 1533 and refs. therein.
6 S. S. Pathaneni and G. R. Desiraju, *J. Chem. Soc., Dalton Trans.*, 1993, 319.
7 R. J. Puddephatt, *Comprehensive Organometallic Chemistry*, 1st edn., eds. G. Wilkinson, F. G. A. Stone and E. W. Abel, Pergamon, Oxford, 1984, vol. 2, p. 765.
8 R. V. Parish and S. M. Cottrill, *Gold Bull.*, 1987, **20**, 3.
9 A. K. H. Al-Sa'ady, K. Moss, C. A. McAuliffe and R. V. Parish, *J. Chem. Soc., Dalton Trans.*, 1984, 1609; P. J. Sadler, *Adv. Inorg. Chem.*, 1991, **36**, 1 and refs. therein.
10 V. W.-W. Yam, C.-L. Chan and K.-K. Cheung, *J. Chem. Soc., Dalton Trans.*, 1996, 4019; S. D. Hanna and J. I. Zink, *Inorg. Chem.*, 1996, **35**, 297.
11 Y. Jiang, S. Alvarez and R. Hoffmann, *Inorg. Chem.*, 1985, **24**, 749; M. J. Calhorda and L. F. Veiros, *J. Organomet. Chem.*, 1994, **478**, 37; P. Pyyko, J. Li and N. Runeburg, *Chem. Phys. Lett.*, 1994, **218**, 133; N. Kaltsoyannis, *J. Chem. Soc., Dalton Trans.*, 1997, 1.
12 W. B. Jones, J. Yuan, R. Narayanaswarmy, M. A. Young, R. C. Elder, A. E. Bruce and M. R. M. Bruce, *Inorg. Chem.*, 1995, **24**, 37.
13 S. Akerstrom, *Ark. Kemi*, 1959, **14**, 387.
14 J. Dobrowolski, Z. Badowski and I. Kwiatkovska, *Rocz. Chem.*, 1976, **50**, 53.
15 H. J. Blaauw, R. J. Nivard and G. J. M. van der Kerk, *J. Organomet. Chem.*, 1964, **2**, 236.
16 F. Forghiera, C. Preti, L. Tassi and G. Tosi, *Polyhedron*, 1988, **7**, 1231.
17 J. B. Miller and J. L. Burmeister, *Synth. React. Inorg. Metal-Org. Chem.*, 1976, **50**, 53; H. J. A. Blaauw, R. J. Nivard and G. J. M. van der Kerk, *J. Organomet. Chem.*, 1964, **2**, 236.
18 L. Schröter and J. Strähle, *Chem. Ber.*, 1991, **124**, 2161.
19 G. E. Coates, C. Kowala and J. M. Swan, *Aust. J. Chem.*, 1966, **19**, 539.
20 E. Delgado and E. Hernandez, *Polyhedron*, 1992, **124**, 2161; R. Narayanaswarmy, M. A. Young, E. Parkhurst, M. Oullette, M. E. Kerr, D. M. Ho, R. C. Elder, A. E. Bruce and M. R. M. Bruce, *Inorg. Chem.*, 1993, **32**, 2506.
21 M. Nakamoto, W. Hiller and H. Schmidbaur, *Chem. Ber.*, 1993, **126**, 605.
22 R. Hesse and P. Jennische, *Acta Chem. Scand.*, 1972, **26**, 3855.
23 P. Jennische, H. Anacker-Eickhoff and A. Wahberg, *Acta Chem. Scand.*, 1975, **31**, 5143.
24 W. Schneider, A. Bauer and H. Schmidbaur, *Chem. Ber.*, 1997, **130**, 641.
25 N. Carr, J. G. Crossley, A. J. Dent, J. R. Gouge, G. N. Greaves, P. S. Jarrett and A. G. Orpen, *J. Chem. Soc., Chem. Commun.*, 1990, 1369.
26 H. Bertagnolli and T. S. Ertel, *Angew. Chem., Int. Ed. Engl.*, 1994, **33**, 45.
27 M. A. Mazid, M. T. Razi, P. J. Sadler, G. N. Greaves, S. J. Gurmon, M. H. J. Koch and J. C. Phillips, *J. Chem. Soc., Chem. Commun.*, 1980, 1261; R. C. Elder, K. Ludwig, J. N. Cooper and M. K. Eidsness, *J. Am. Chem. Soc.*, 1985, **107**, 5024.
28 See, for example, A. K. Brisdon, J. M. Holloway, E. G. Hope, W. Leveson, J. S. Ogden and A. K. Saad, *J. Chem. Soc., Dalton Trans.*, 1992, 447.
29 S. J. Guman, N. Binsted, J. W. Campbell and I. Ross, *J. Phys. Chem.*, 1984, **17**, 143; 1986, **19**, 1845.
30 R. W. Joyner, K. J. Martin and P. Meehan, *J. Phys. Chem.*, 1987, **20**, 4005.
31 D. D. Perrin, D. R. Perrin and W. L. F. Armitage, *Purification of Laboratory Chemicals*, 2nd edn., Pergamon, Oxford, 1980.
32 E. Biilman, *Liebigs Ann. Chem.*, 1906, **348**, 120.
33 DIFABS, N. Walker and D. Stewart, *Acta Crystallogr., Sect. A*, 1983, **39**, 158.
34 G. M. Sheldrick, *Acta Crystallogr., Sect. A*, 1990, **46**, 467.
35 G. M. Sheldrick, SHELXL 93, a Computer Program for Crystal Structure Refinement, University of Göttingen, 1993.
36 P. McArdle, *J. Appl. Crystallogr.*, 1994, **27**, 438.

Received 23*rd October* 1997; *Paper* 7/07650I